Supplementary Information

Microtomy-fabricated two-dimensional nano-slits enable single molecule biosensing

Muhammad Sajeer P[a,b,c,d], Ankit Bhardwaj[b,d], Boya Radha[b,d,e*], Manoj Varma[c*] and Ashok Keerthi [a,d,e*]

[a]Department of Chemistry, School of Natural Sciences, The University of Manchester, Manchester M13 9PL, UK

[b]Department of Physics and Astronomy, School of Natural Sciences, The University of Manchester, Manchester, M13 9PL, UK

[c]Center for Nanoscience and Engineering, Indian Institute of Science, 560012, India

[d]National Graphene Institute, The University of Manchester, Manchester, M139PL, UK.

[e]Photon Science Institute, The University of Manchester, Manchester M13 9PL, UK

* ashok.keerthi@manchester.ac.uk, radha.boya@manchester.ac.uk, mvarma@iisc.ac.in

Contents:

1. Methods – Ultramicrotomy-fabricated MoS_2 based 2D nano-slits

The method for fabricating 2D channels devices described here has been previously published[1], where we demonstrated its effectiveness in producing precise 2D materials channel structures. This well-established technique involves mechanical exfoliation, wet transfer, and van der Waals assembly, followed by resin embedding and sectioning. In brief, 2D crystal flakes of MoS_2 were prepared via mechanical exfoliation. These flakes were transferred onto silicon dioxide (SiO_2) substrates using a wet transfer method, which involved etching SiO_2 in aqueous KOH. Ultra-flat resin blocks were prepared as substrates for these 2D crystals or stacks by casting epoxy resin into a PDMS mold replicating a silicon wafer's surface. These resin blocks provided a stable and smooth platform for transferring the 2D crystals or stacks.

To fabricate slit-shaped 2D channels, a van der Waals assembly was employed by stacking three exfoliated layers: top, bottom, and spacer layers. The top and bottom layers were 500 nm thick, while the spacer layer was around 8.4 nm. The spacer layer was made using electron beam lithography and dry etching techniques. The prepared stack were embedded in resin and sectioned using an ultramicrotome for subsequent analysis and device fabrication. Please refer to reference 1 for detailed experimental procedure for device fabrication.

2. Power Spectral Density (PSD) analysis

The DNA transloation data using Axopatch 200B is aquired using custom LABVIEW software. The translocaion data is acquired as 10kb files each, for entire acquisition time of the experiment. One of this time domain data file is used for the plotting using Power Spectral Densities using Transalyzer MATLAB software package. The figure S1 shows the flicker noise regime of ionic current signal. This noise is typically assosiated with mobility of ionic charge carrier, bubbles, electrode noise, and ion aggregations near channel[2,3].

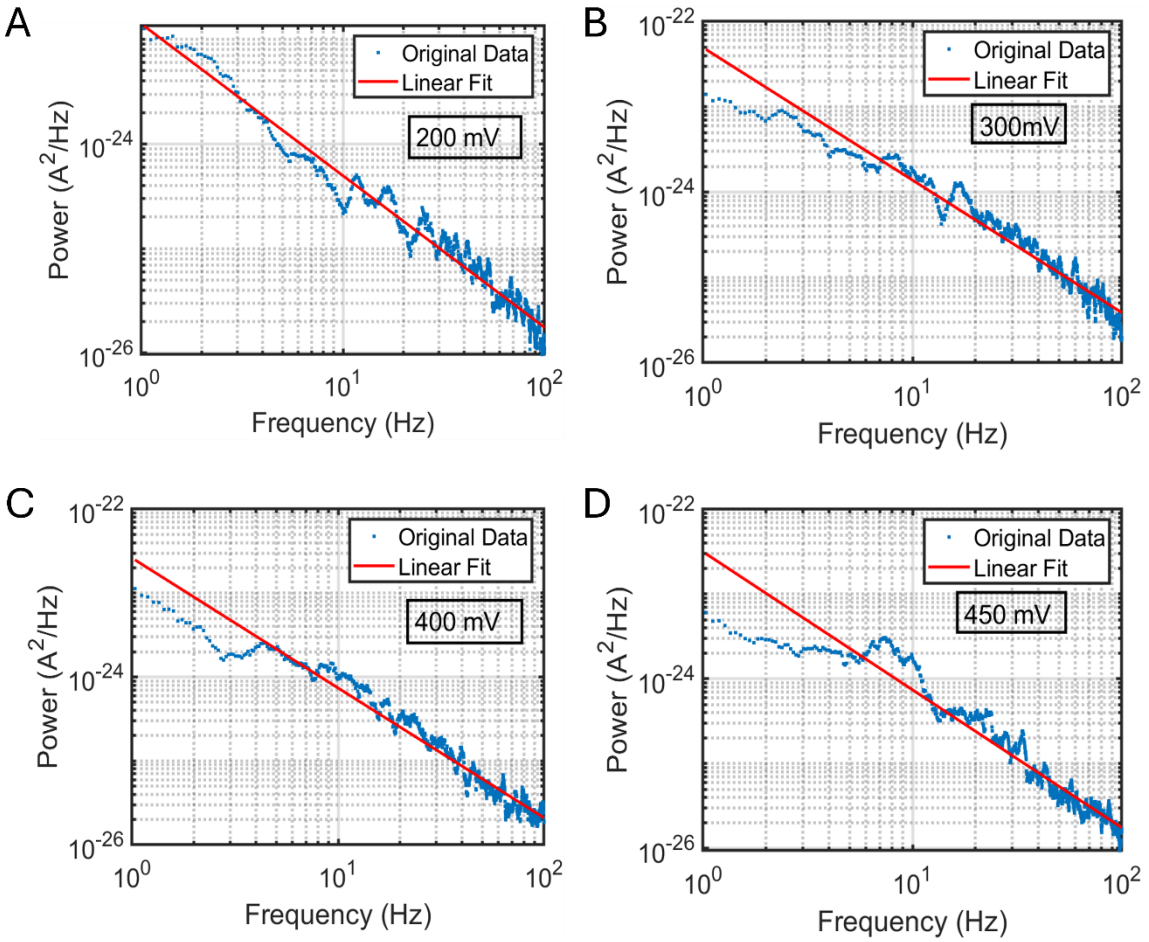

Figure S1. The linear fitting of PSD diagram using polyfit function in MATLAB to find the exponent. We have used 4 M LiCl with different voltages ranges, 200 mV (A), 300 mV (B), 400 mV (C) and 450 mV (D). The exponent varies from 1.4 to 1.6 (the average value is 1.5). The corresponding MATLAB code is available in GitHub profile.

3. Device stability before and after DNA sensing measurements

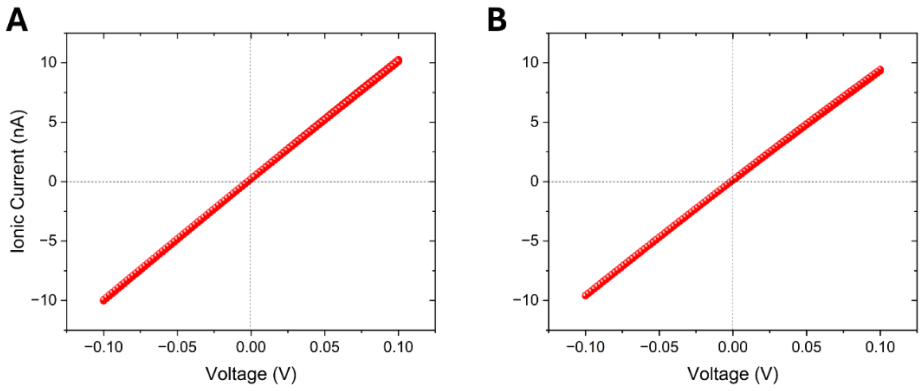

Figure S2. Current *vs* voltage (I–V) characteristics of the MoS_2 2D nano-slit device in 4 M KCl aqueous electrolyte, measured before (A) and after (B) DNA translocation experiments. These I–V curves show no significant change, indicating that there was no clogging of the 2D nano-slits or adhesion of biopolymers to the channel surfaces during the measurements.

4. Opening of 2D nano-slit device

Right after fabrication of 2D nano-slit device, we open channels and make the device conductive for ion transport. This is achieved *via* repeated cycling (repeated I-V cycles in 0.1 M KCl aqueous electrolyte) as we explained in our previous work[4]. A gradual opening of channel with 0.1M KCl is given in Figure S3. After channels are fully open, I-V is recorded in 1 M KCl aqueous electrolyte which shown in Figure S4.

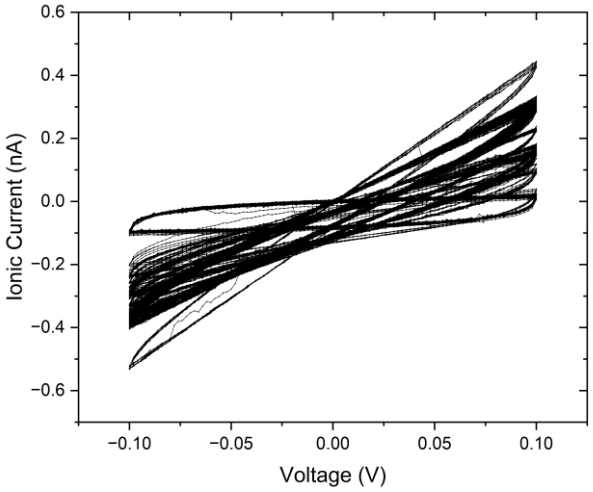

Figure S3. Gradual opening of 2D nano-slit channel device. The current-voltage (I-V) curves of MoS_2 2D nano-slit in 0.1M KCl aqueous electrolyte across multiple cycles. This graph shows the gradual increase in ionic current indicating a slow opening of the nano-slit channel.

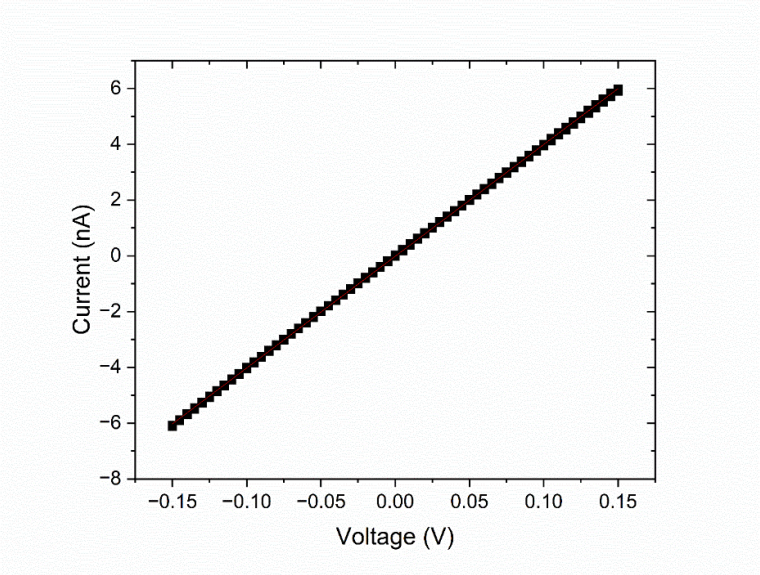

Figure S4. Current-voltage (I-V) curve of MoS_2 2D nano-slit in 1 M KCl aqueous electrolyte. The theoretical conductance for 1 M KCl is 0.26×10^{-7} S whereas measured conductance from our device is 0.40×10^{-7} S.

5. Additional DNA translocation data

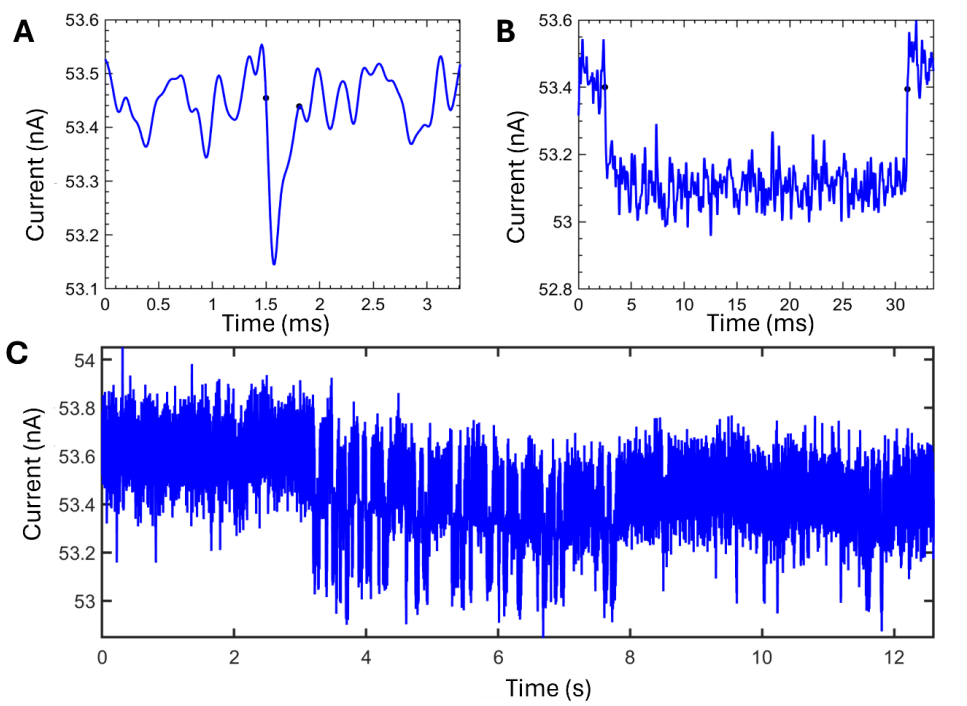

Figure S5. The DNA translocation data at 450 mV using 4 M LiCl electrolyte. A) A representative spike event, with a blockade amplitude of 0.29 and dwell time of 0.12 ms. B) A representative DNA translocation event through the channel, with a current blockade amplitude of 0.28 and dwell time of 28.4 ms. C) The recorded ionic current trace at 450 mV over 12 seconds.

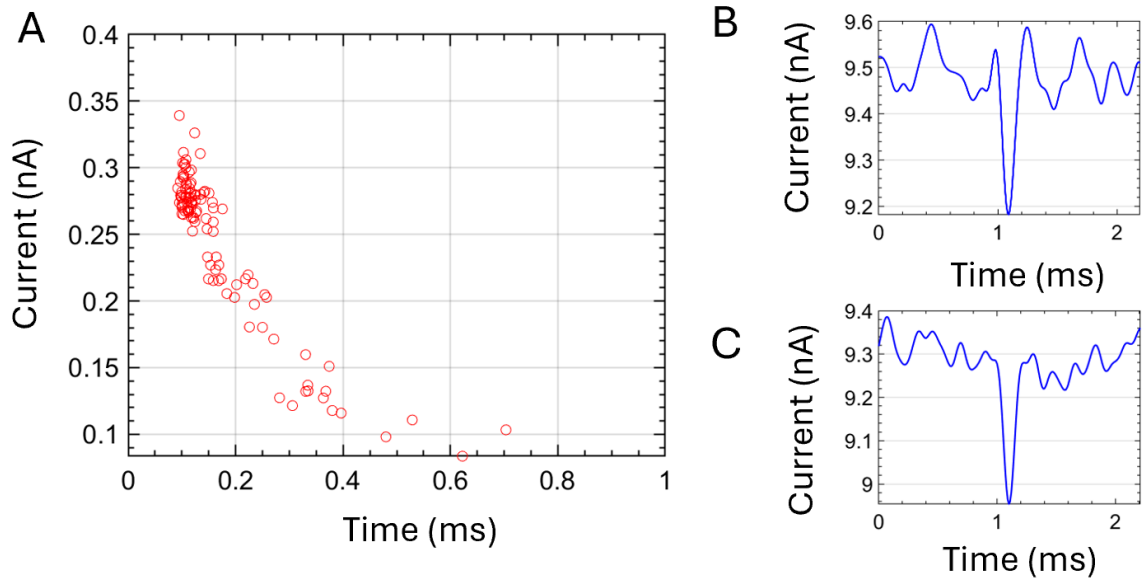

Figure S6: A) The current blockade *vs* dwell time graph of spike events of DNA (5 kbp linear dsDNA) translocation at 100 mV through MoS_2 based 2D nano-slit devices. B) and C) Representative figures of the spike events.

6. DNA Topology investigations

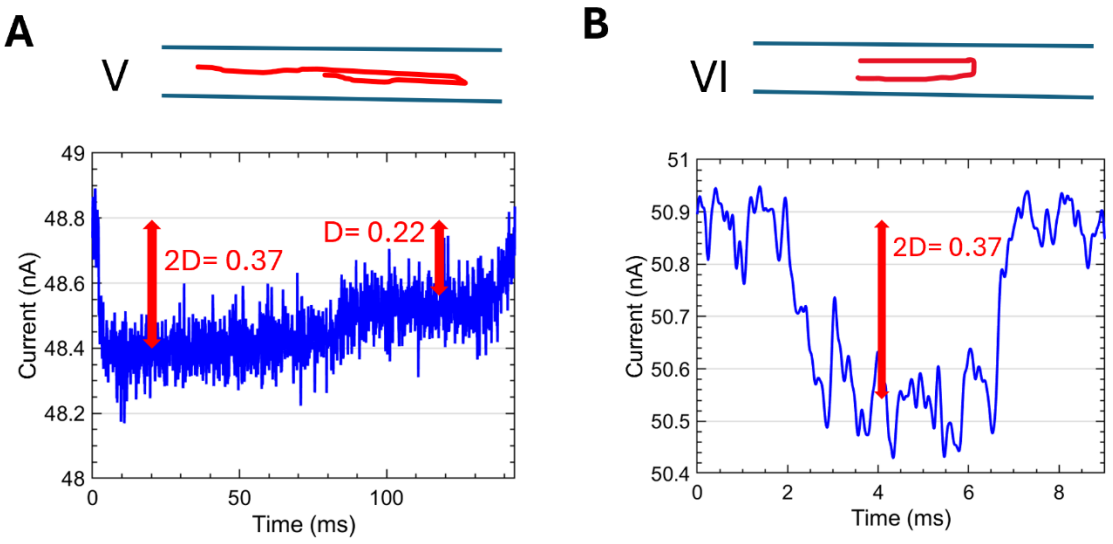

Figure S7: Comparison of depth of current blockade signal for representative DNA folding. A single strand represents a current blockade of D = 0.22 nA, while double folded DNA represent approximately double current blockade, ~2D = 0.37 nA, confirming the folding of DNA.

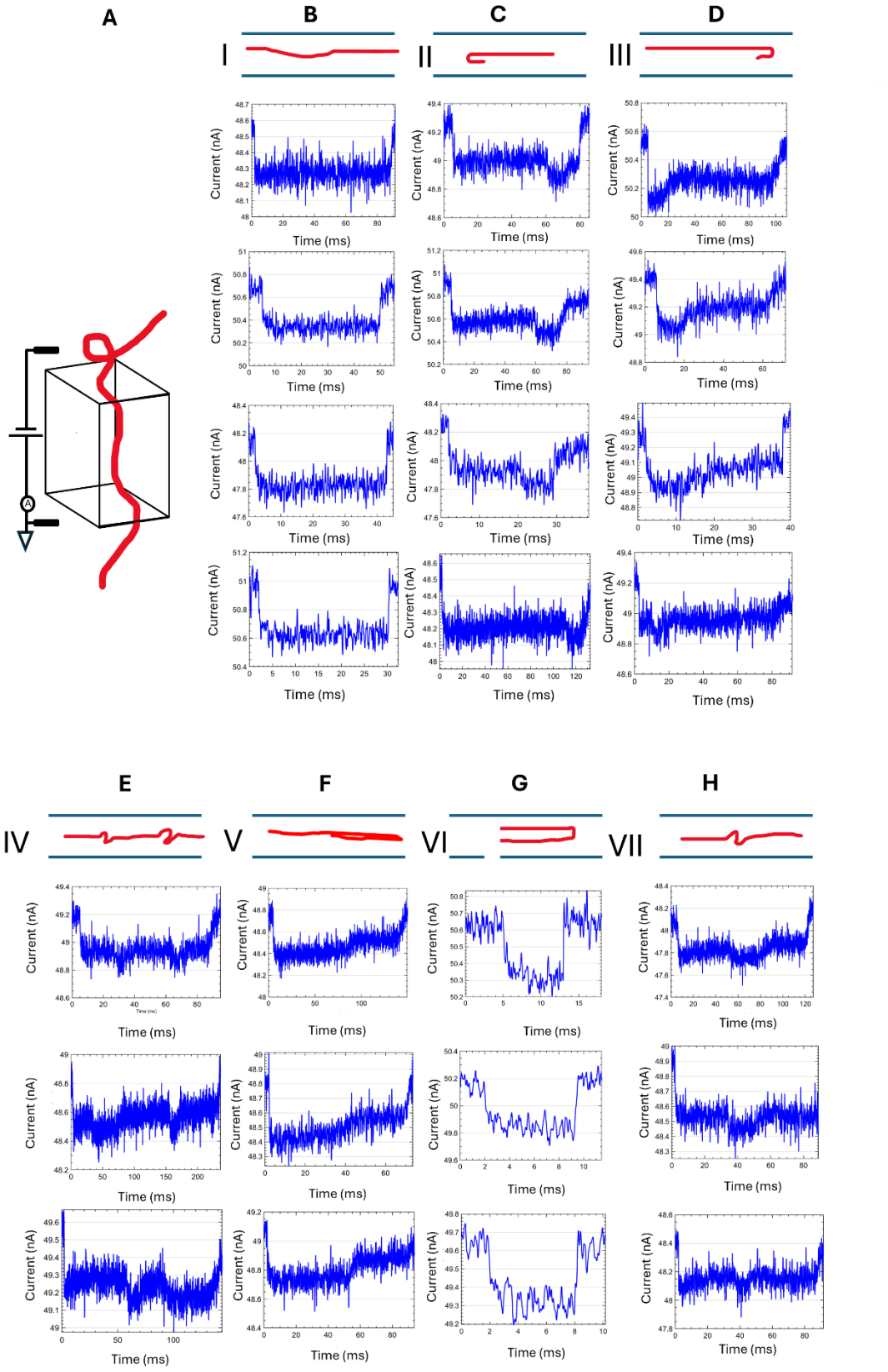

Figure S8: A) Schematic of DNA translocating through a 2D nano-slit. B) – H) Nano-slit microscopy for understanding the topology of DNA folding types and corresponding current blockade signals. (I) Unfolded DNA, (II) semi folded DNA at left-end, (III) semi folded DNA on the right-end, (IV) two-times bent configuration in DNA, (V) partially folded DNA, (VI) fully folded DNA configurations and (VII) bent or partially folded DNA conformation.

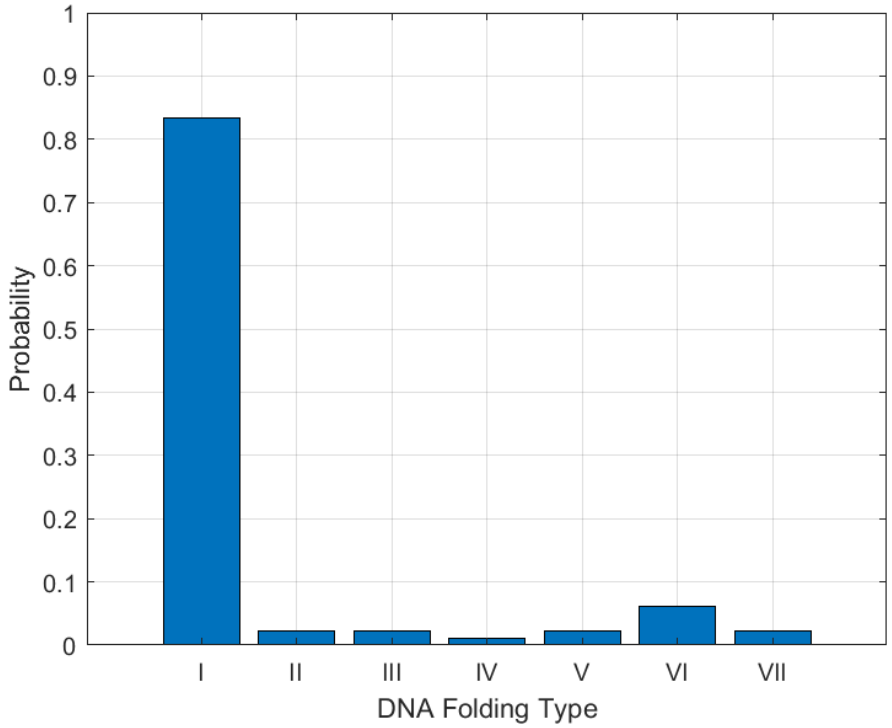

Figure S9: The probability distribution of different DNA folding types. The corresponding folding types are as shown in Figure S8.

7. References

1. Bhardwaj, A. *et al.* Ultramicrotomy-Assisted Fabrication of Nanochannels for Efficient Ion Transport and Energy Generation. *Adv. Funct. Mater.* 2401988 (2024) doi:10.1002/adfm.202401988.

2. Fragasso, Alessio, Sonja Schmid, and Cees Dekker. "Comparing current noise in biological and solid-state nanopores." ACS nano 14, no. 2 (2020): 1338-1349.

3. Wu, Lingzhi, Hang Liu, Wenyuan Zhao, Lei Wang, Chuanrong Hou, Quanjun Liu, and Zuhong Lu. "Electrically facilitated translocation of protein through solid nanopore." Nanoscale Research Letters 9 (2014): 1-10.

4. Goutham, Solleti, Raj Kumar Gogoi, Hiran Jyothilal, Gwang-Hyeon Nam, Abdulghani Ismail, Siddhi Vinayak Pandey, Ashok Keerthi, and Boya Radha. "Electric Field Mediated Unclogging of Angstrom-Scale Channels." *Small Methods* 9, no. 3 (2025): 2400961.